

Magnetic Properties of an Antiferromagnet CePdSb₃

Arumugam THAMIZHAVEL¹, Hiroshi NAKASHIMA¹, Tomoyuki SHIROMOTO¹,
Yoshiko OBIRAKI¹, Tatsuma D MATSUDA², Yoshinori HAGA², Srinivasan
RAMAKRISHNAN³, Tetsuya TAKEUCHI⁴, Rikio SETTAI¹ and Yoshichika ŌNUKI^{1,2}

¹*Graduate School of Science, Osaka University, Toyonaka, Osaka 560-0043*

²*Advanced Science Research Center, Japan Atomic Energy Research Institute,
Tokai, Ibaraki 319-1159*

³*Tata Institute of Fundamental Research, Homi Bhabha Road, Colaba, Mumbai 400-005, India*

⁴*Low Temperature Center, Osaka University, Toyonaka, Osaka 560-0043*

(Received June 29, 2005)

We report the resistivity, magnetic susceptibility, magnetization and specific heat studies on a single crystal of CePdSb₃ which crystallizes in the orthorhombic crystal structure. CePdSb₃ behaves as a Kondo lattice compound in which Ce moments order antiferromagnetically below 3.1 K, in contrast to the previously published polycrystal data. The magnetic susceptibility is highly anisotropic, reflecting the orthorhombic crystal structure. The magnetization for $H \parallel [001]$, which corresponds to the easy axis, shows a metamagnetic transition at 1.6 kOe and saturates above 10 kOe, reaching a value of $1.6 \mu_B/\text{Ce}$. The magnetization for $H \parallel [010]$ also shows a metamagnetic transition at 11 kOe, while the magnetization $H \parallel [100]$ increases linearly as a function of magnetic field, indicating a hard axis.

KEYWORDS: Antiferromagnetism, Kondo lattice, CePdSb₃, metamagnetic

1. Introduction

The f electrons of rare earth and uranium compounds exhibit a variety of characteristic features including spin and valence fluctuations, spin and charge orderings, heavy fermion and anisotropic superconductivity.^{1,2} Of all the rare-earth intermetallic compounds studied so far, the Sb containing intermetallic compounds have been found to exhibit a variety of interesting physical properties. The equiatomic ternary compound CeRhSb, which crystallizes in the orthorhombic crystal structure, is a semiconductor-type valence fluctuating compound.³ On the other hand, CePdSb crystallizes in the hexagonal GaGeLi structure (P6₃mc) and exhibits a Kondo lattice property in its transport properties, together with a ferromagnetic ground state, with a moment of $1.2 \mu_B/\text{Ce}$ lying in the basal plane.⁴ CeT₄Sb₁₂ (T: transition metal) skutterudite compounds show semiconductive behavior, which is attributed to the large $c - f$ hybridization strength originating from their unique crystal structure. The skutterudite PrOs₄Sb₁₂ is found to be a heavy fermion superconductor below $T_c = 1.8 \text{ K}$,⁵ which is one of the very few examples of multiphase superconductivity.

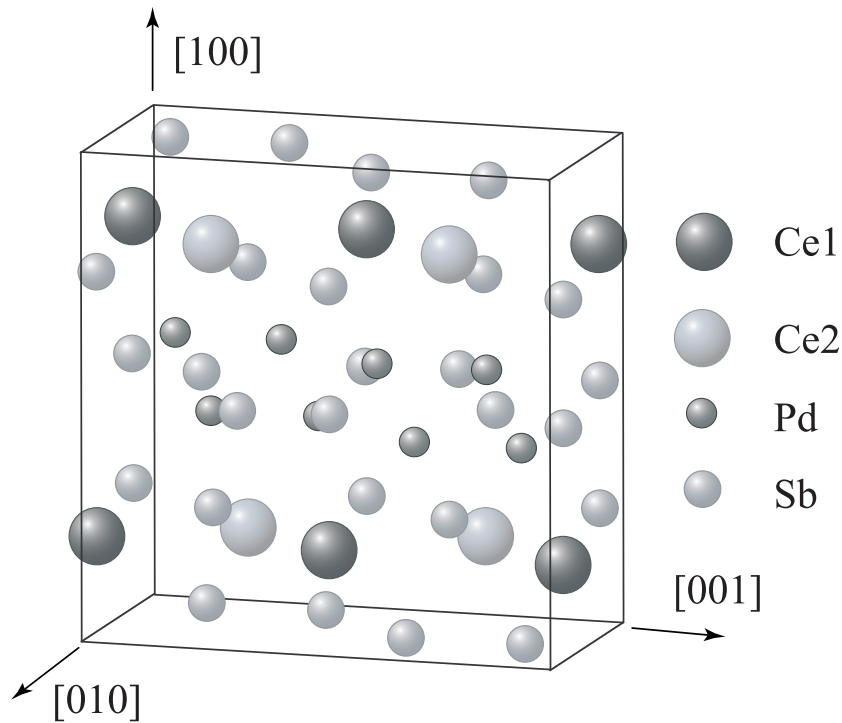
Recently, we have studied a series of CeTSb₂ (T : Cu, Au, Ag and Ni) single crystals,^{6,7} in which CeAgSb₂ indicated ferromagnetic ordering below $T_C = 9.6$ K. However, the magnetization for the field along the [001] tetragonal direction indicated a typical ferromagnetic response with a saturation moment $\mu_s \simeq 0.4\mu_B/\text{Ce}$, while the magnetization for $H \parallel [100]$ increased almost linearly up to 3 T and showed a saturation feature at higher fields, reaching $1.15\mu_B/\text{Ce}$ at 5 T. The de Haas van-Alphen (dHvA) effect measurement on CeAgSb₂ revealed large dHvA frequencies of 10^8 Oe, which corresponded to cylindrical Fermi surfaces for the magnetic field along the [001] direction, indicating the quasi-two-dimensional electronic state. The dHvA branches in CeAgSb₂ were highly different from those with small dHvA frequencies of 10^7 Oe in a reference compound LaAgSb₂. It was concluded that the $4f$ electrons are localized and the Fermi surface of CeAgSb₂ is similar to that of LaAgSb₂, except for a slight enlargement which enables it to form the large orbits along a hollow cylindrical Fermi surface.⁸

With all these interesting properties and in continuation to our research on the ternary rare-earth intermetallic antimony containing compounds, we have successfully grown the single crystals of CePdSb₃ for the first time using Sb as flux. Previous studies on this compound were done on a polycrystalline sample about a decade ago by Cava *et al.*⁹ in which they reported that CePdSb₃ did not order magnetically. On the other hand, the present studies on the flux-grown single crystals revealed a clear antiferromagnetic ordering at $T_N = 3.1$ K. In this paper, we report on the electrical resistivity, magnetic susceptibility, magnetization and specific heat studies on a single crystal of CePdSb₃. The magnetic anisotropy is discussed on the basis of the crystalline electric field (CEF) scheme.

2. Experimental details

A sample of CePdSb₃ was made by melting the individual constituents (taken in stoichiometric proportions) in an arc furnace under high-purity argon atmosphere. The purity of the Ce and Pd metals was 99.9 % and 99.99 %, respectively, whereas the purity of Sb was 99.999 %. The alloy buttons were remelted four times to ensure proper mixing. This alloy was mixed with excess Sb and placed in a high density alumina crucible, which is then sealed inside an evacuated quartz ampoule with a partial pressure of Ar. The temperature of the furnace was increased up to 1000 °C in two days and the mixture was kept at this temperature for further two days in order to attain proper homogenization. Subsequently, the furnace was cooled down to 650 °C over a period of three weeks and then rapidly to room temperature. Single crystals in the form of shining platelets were obtained in this process. The high quality of the crystals was ascertained using the X-ray Laue back reflection technique, which showed a pattern of Laue spots belonging to the orthorhombic unit cell.

The crystal structure was determined by the single crystal X-ray diffraction. A very small single crystal of CePdSb₃ having approximate dimensions of $0.1 \times 0.1 \times 0.1$ mm³ was mounted

Fig. 1. Crystal structure of CePdSb₃.Table I. Atomic positions and isotropic displacement parameters for CePdSb₃.

Atom	Wyckoff position	x	y	z	B_{eq}
Ce1	$4c$	0.198120	0.75	0.50	0.578(6)
Ce2	$4d$	0.19103(3)	0.22229(6)	0.75	0.558(6)
Pd	$8e$	0.39649(3)	0.45237	0.63426	0.749(7)
Sb1	$8e$	0.00352(3)	0.48553(5)	0.62254(2)	0.713(6)
Sb2	$4c$	0.26294(4)	0.25	0.5	0.638(8)
Sb3	$4c$	0.52621(4)	0.25	0.5	0.725(8)
Sb4	$4d$	0.27238(4)	0.76534(7)	0.25	0.694(8)
Sb5	$4d$	0.43700(4)	0.07720(7)	0.7500	0.662(8)

on a glass fiber and the measurements were made using a Rigaku RAXIS RAPID imaging plate area detector with graphite monochromated Mo-K α radiation. The lattice constants and an orientation matrix for data collection corresponded to the orthorhombic unit cell with space group $Pbcm$ (# 57) and lattice parameters $a = 12.780$ Å, $b = 6.330$ Å and $c = 12.453$ Å. The crystal structure of CePdSb₃ is shown in Fig. 1. The atomic positions and displacement parameters are listed in Table I. It is to be mentioned here that recently Macaluso *et al.*¹⁰ have reported the detailed crystal structure of an isotypic CeNiSb₃ single crystal, which also

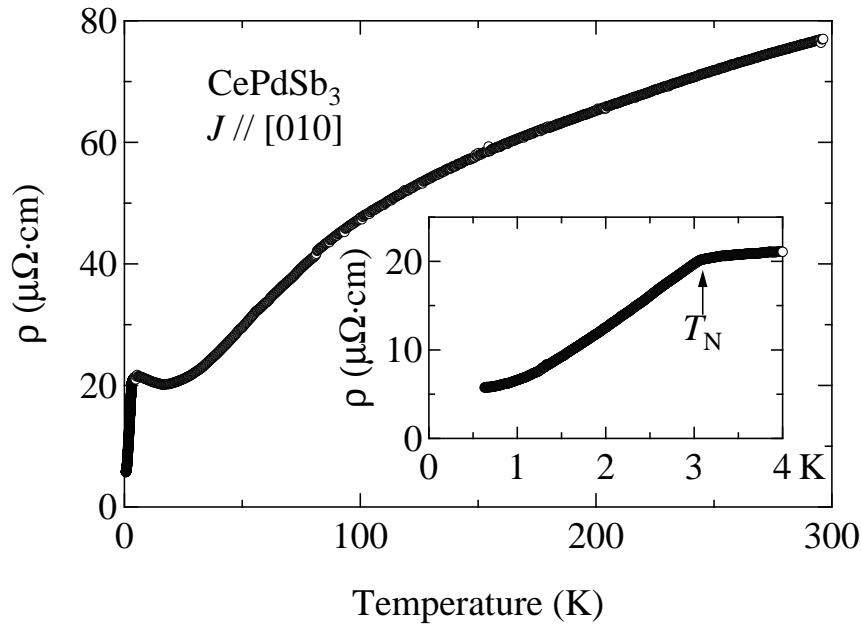


Fig. 2. Temperature dependence of the electrical resistivity of CePdSb₃. The inset shows the low-temperature resistivity data.

crystallizes in the orthorhombic crystal structure with the same space group $Pbcm(\# 57)$, although the Wyckoff positions are different between CeNiSb₃ and CePdSb₃.

The temperature dependence of the magnetic susceptibility and magnetization were measured using a commercial SQUID magnetometer in the temperature range from 1.9 to 300 K. The electrical resistivity was measured using a four-probe DC technique. The specific heat between 0.67 and 10 K was measured using a quasi-adiabatic heat-pulse calorimeter.

3. Experimental Results

3.1 Electrical resistivity

The temperature dependence of the resistivity ρ for the current J along the [010] direction is shown in Fig. 2. The inset shows the low-temperature resistivity data. The temperature dependence of the electrical resistivity clearly reveals that the electrical resistivity has a broad peak around 100 K, has a minimum value around 16 K, increases up to about 3 K, and starts to decrease rapidly below a Néel temperature of $T_N = 3.1$ K, which will be clarified in a next section. Such a feature of the resistivity agrees with the notion of the presence of the Kondo effect in this sample.¹¹ The inset shows a distinct anomaly in the resistivity at $T_N = 3.1$ K due to the antiferromagnetic ordering of Ce moments. The temperature dependence of resistivity below 2 K obeys the Fermi liquid relation $\rho = \rho_0 + AT^2$. The A and ρ_0 values thus obtained by fitting to the above equation are $A = 1.89 \mu\Omega\cdot\text{cm}/\text{K}^2$ and $\rho_0 = 4.86 \mu\Omega\cdot\text{cm}$.

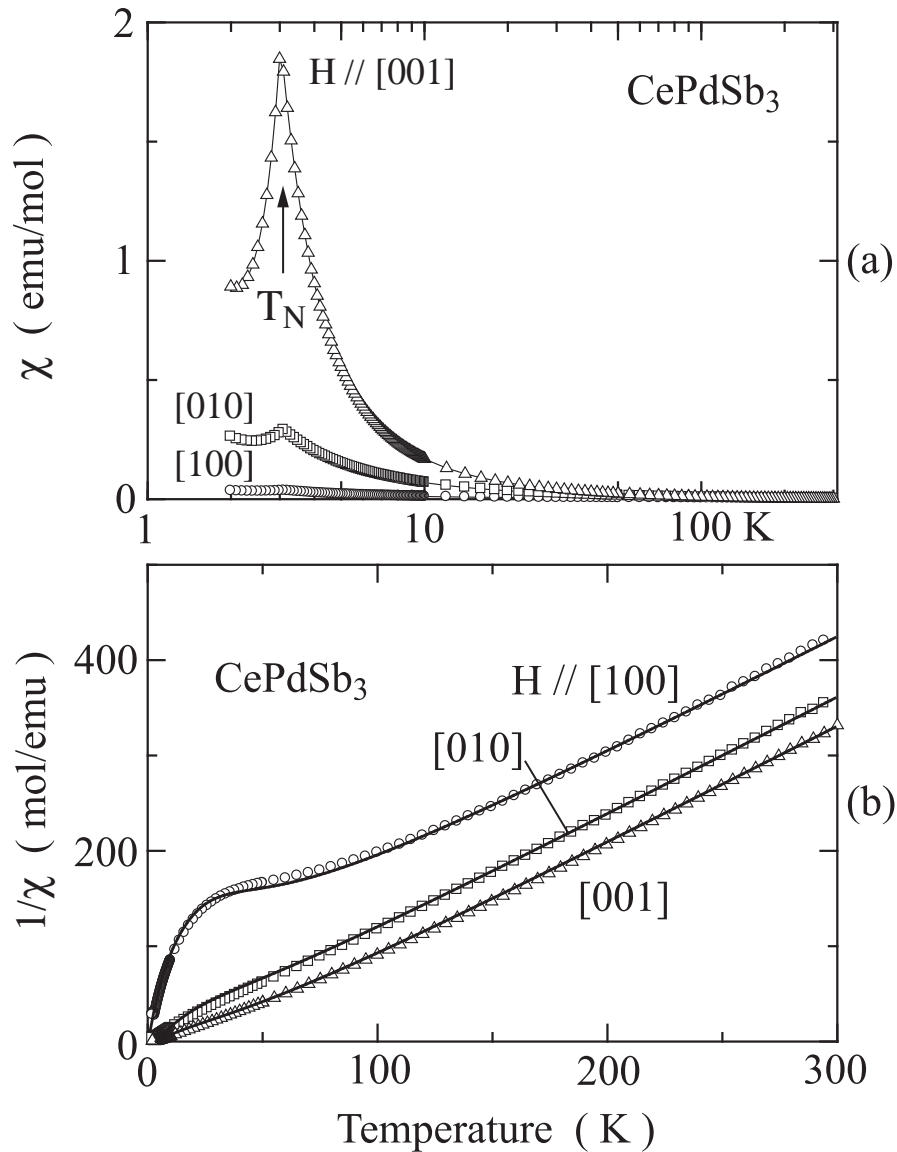


Fig. 3. (a) Temperature dependence of the magnetic susceptibility χ from 1.9 to 300 K in semi-logarithmic scale and (b) the inverse magnetic susceptibility plot of CePdSb₃. Solid lines in (b) are the results of CEF calculations.

3.2 Magnetic susceptibility and magnetization

The temperature dependence of the magnetic susceptibility χ for three principal directions is shown in Fig. 3. The magnetic susceptibility has been measured in a magnetic field of 10 kOe for all the directions. From Fig. 3(a), one can clearly see a steep decrease of the susceptibility below $T_N = 3.1$ K due to the antiferromagnetic ordering of Ce moments, especially for $H \parallel [001]$. The [001] direction is estimated to be an easy-axis, while the hard axis corresponds to [100]. Figure 3(b) shows the inverse susceptibility plot. As one can see from the figure, the inverse susceptibility follows the Curie-Weiss law at high temperatures with an

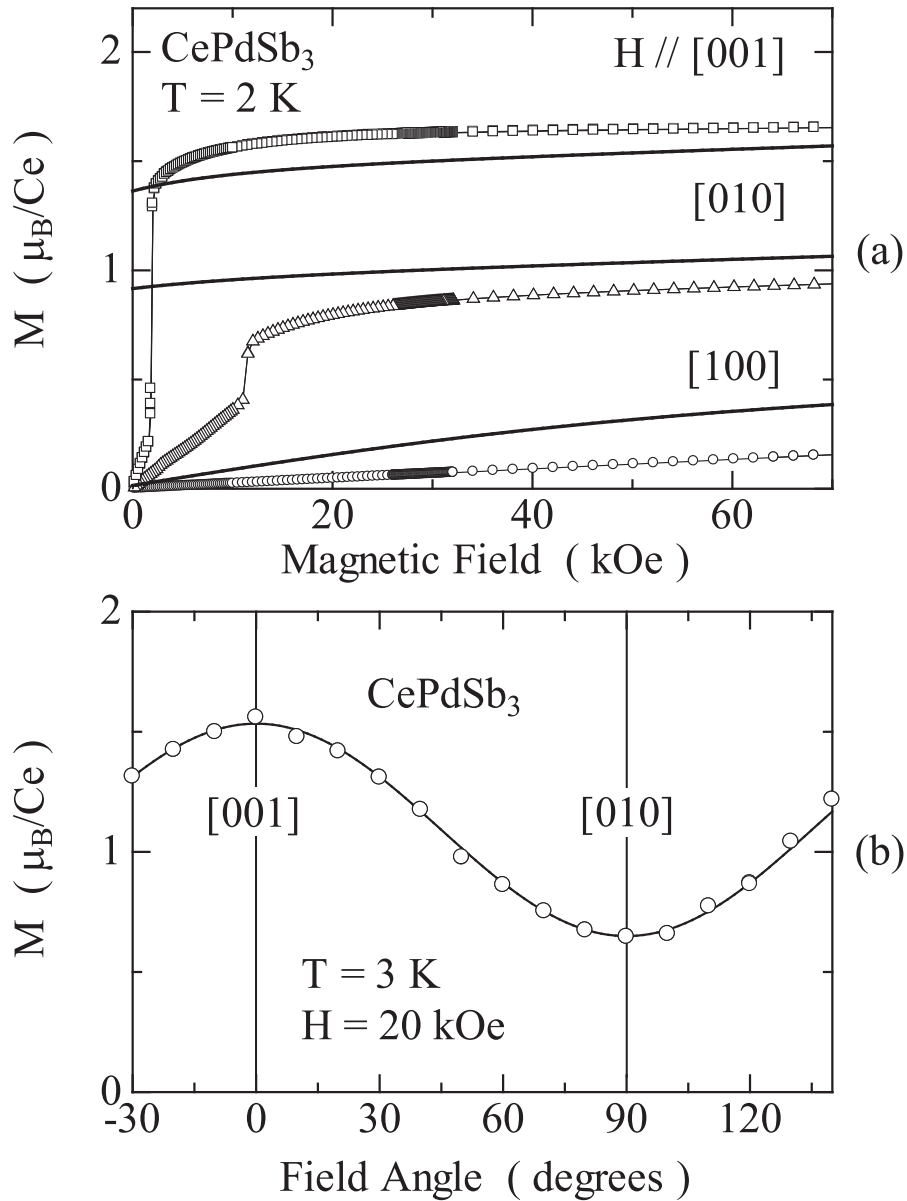


Fig. 4. (a) Isothermal magnetization M of CePdSb_3 vs. magnetic field H at $T = 2 \text{ K}$ for the three crystallographic directions and (b) the angular dependence of magnetization at 3.0 K in a field of 20 kOe . Thick solid lines in (a) are calculated CEF magnetization curves.

effective magnetic moment of $2.54 \mu_B/\text{Ce}$. The inverse susceptibility for $H \parallel [010]$ and $[001]$ indicates rather linear temperature dependence, while that for $H \parallel [100]$ shows a pronounced shoulder like feature around 25 K . This anisotropy is probably due to the crystalline electric field (CEF) effect. Solid lines in Fig. 3(b) are the calculated curves based on a CEF model, which will be discussed later.

The field dependence of the isothermal magnetization M is shown in Fig. 4. It is obvious from the figure that the isothermal magnetization curves are qualitatively different for the

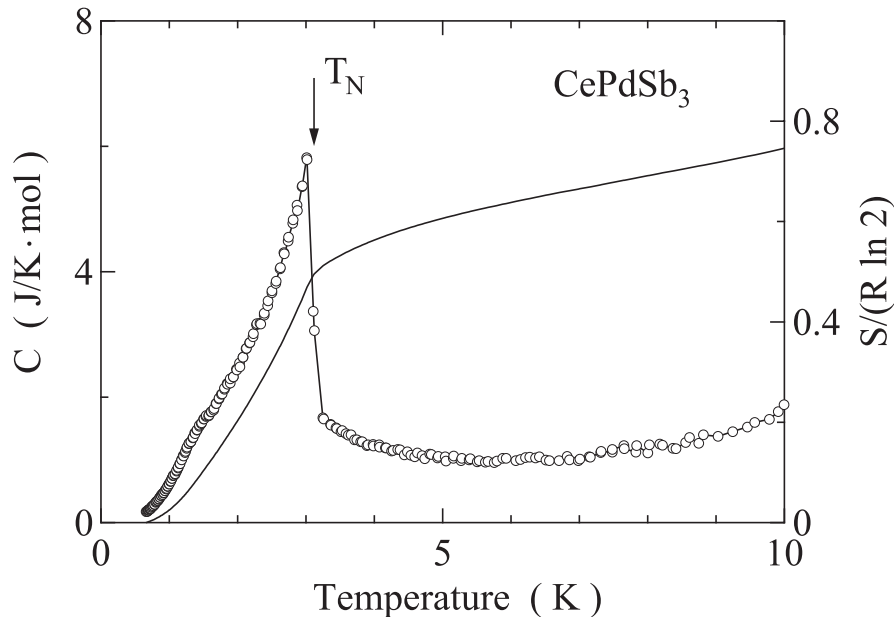


Fig. 5. Temperature dependence of the specific heat and entropy in CePdSb_3 .

three orientations, showing a strong anisotropy. As can be seen from the figure, the magnetization for $H \parallel [001]$ indicates a metamagnetic transition at a low applied field, which further substantiates the antiferromagnetic ordering of this compound. The metamagnetic transition occurs at an applied field of 1.6 kOe. With further increasing the applied field, the magnetization reaches a saturation value of about $1.6 \mu_B/\text{Ce}$, indicating that the $[001]$ direction is the easy axis of the magnetization. For $H \parallel [010]$, a metamagnetic transition is seen at 11 kOe and the magnetization saturates for higher applied magnetic fields. The magnetization along the $[100]$ direction increases linearly without any metamagnetic transitions, indicating that the $[100]$ direction is the hard axis of magnetization. The solid lines in Fig. 4(a) are the calculated magnetization curves based on a CEF model which will be described in the next section.

We have also plotted the angular dependence of magnetization in a field of 20 kOe at 3 K. This plot indicates that the magnetization for $H \parallel [001]$ decreases smoothly from the saturated value of $1.6 \mu_B/\text{Ce}$ as the field angle is tilted towards the $[010]$ direction and then again smoothly increases. This angular dependence of magnetization further substantiates the magnetization measurement shown in Fig. 3(a).

3.3 Specific heat

The temperature dependence of the specific heat C in the temperature range from 0.67 to 10 K is shown in Fig. 5. The jump in the heat capacity data clearly shows the bulk magnetic ordering of Ce^{3+} moments at $T_N = 3.1$ K. Although the transition at 3.1 K is very sharp, the value of the total entropy at T_N is only $0.5R \ln 2$. This implies that there might be a significant

contribution to the heat capacity at higher temperatures, which is based on the short-range antiferromagnetic ordering above T_N and/or the Kondo effect as seen from the resistivity data. Here we estimated the magnetic entropy under the assumption that the specific heat C corresponds to the magnetic specific heat C_{mag} , simply neglecting a phonon contribution to the specific heat. Also, here we note that we could not determine the electronic specific heat coefficient γ from the low temperature specific heat data because of the fact that the estimation of γ by the usual method of extrapolating the C/T vs T^2 plot results in a very small value with γ value nearly equal to zero.

4. Analyses and Discussion

Here we try to analyze the magnetic susceptibility and magnetization data by using a CEF model. First of all, we should discuss the crystal structure of CePdSb₃. As shown in Table I, there are two Ce sites in this compound with the Wyckoff positions of $4c$ and $4d$, respectively. These two sites have monoclinic symmetry, although the crystal structure is orthorhombic. Therefore, we basically should consider the two Ce sites with the monoclinic site symmetry for the CEF calculation. This brings about a complicated parameter fitting procedure. In order to perform a tentative analysis on the basis of the CEF model, here we assume only one site for the Ce atoms in the following calculation.

The CEF Hamiltonian for the monoclinic site symmetry is written as

$$\mathcal{H}_{\text{CEF}} = B_2^0 \mathbf{O}_2^0 + B_2^2 \mathbf{O}_2^2 + B_2^{-2} \mathbf{O}_2^{-2} + B_4^0 \mathbf{O}_4^0 + B_4^2 \mathbf{O}_4^2 + B_4^{-2} \mathbf{O}_4^{-2} + B_4^4 \mathbf{O}_4^4 + B_4^{-4} \mathbf{O}_4^{-4}, \quad (1)$$

where B_n^m are the CEF parameters and \mathbf{O}_n^m the Stevens operators.^{12,13} The CEF susceptibility is defined as

$$\chi_{\text{CEF}i} = N(g_J \mu_B)^2 \frac{1}{Z} \left(\sum_{m \neq n} |\langle m | J_i | n \rangle|^2 \frac{1 - e^{-\beta \Delta_{m,n}}}{\Delta_{m,n}} e^{-\beta E_n} + \sum_n |\langle n | J_i | n \rangle|^2 \beta e^{-\beta E_n} \right), \quad (2)$$

where g_J is the Landé g -factor ($= 6/7$ for Ce^{3+}), E_n and $|n\rangle$ are the n th eigenvalue and eigenfunction, respectively. J_i ($i = x, y$ and z) is the component of the angular momentum, and $\Delta_{m,n} = E_n - E_m$, $Z = \sum_n e^{-\beta E_n}$ and $\beta = 1/k_B T$. The magnetic susceptibility including the molecular field contribution λ_i is given by

$$\chi_i^{-1} = \chi_{\text{CEF}i}^{-1} - \lambda_i. \quad (3)$$

We have also calculated the magnetization by using the following formula:

$$M_i = g_J \mu_B \sum_n |\langle n | J_i | n \rangle| \frac{e^{-\beta E_n}}{Z}, \quad (4)$$

where the eigenvalue E_n and the eigenfunction $|n\rangle$ are determined by diagonalizing the total Hamiltonian:

$$\mathcal{H} = \mathcal{H}_{\text{CEF}} - g_J \mu_B J_i (H + \lambda_i M_i), \quad (5)$$

Table II. CEF parameters, energy level schemes and the corresponding wave functions for CePdSb₃.

CEF parameters							
B_2^0 (K)	B_2^2 (K)	B_2^{-2} (K)	B_4^0 (K)	B_4^2 (K)	B_4^{-2} (K)	B_4^4 (K)	B_4^{-4} (K)
6	5	0.5	-0.1	0.2	1.5	0	1
λ_x (mol/emu)	$\lambda_{y,z}$ (mol/emu)						
12	5						
energy levels and wave functions							
E(K)	$ -5/2\rangle$	$ -3/2\rangle$	$ -1/2\rangle$	$ +1/2\rangle$	$ +3/2\rangle$	$ +5/2\rangle$	
174	0	$0.37 + 0.05i$	0	$0.33 + 0.10i$	0	$0.43 - 0.75i$	
174	0.86	0	$0.08 - 0.34i$	0	$0.14 - 0.34i$	0	
96	0	$-0.80 + 0.32i$	0	$-0.17 + 0.26i$	0	$-0.35 + 0.18i$	
96	-0.39	0	$-0.27 - 0.16i$	0	$0.57 - 0.64i$	0	
0	0	$-0.30 - 0.16i$	0	$-0.20 + 0.86i$	0	$-0.21 - 0.25i$	
0	0.32	0	$-0.53 + 0.71i$	0	$0.31 + 0.31i$	0	

where \mathcal{H}_{CEF} is given by eq. (1), the second term is the Zeeman term and the third one is the molecular field.

The CEF parameters were estimated from the fits to the magnetic susceptibility and magnetization data. Solid lines in Figs. 3(b) and 4(a) show the calculated curves by using the CEF parameters listed in Table II. The inverse susceptibility and the anisotropy of the high-field magnetization are well understood by the present CEF model. A saturation moment and large anisotropy in the magnetization can be well explained by this simple model. The high-temperature specific heat and inelastic neutron scattering experiments are desirable for more detailed analyses, which are left for the future study.

It is noted that the γ value is relatively small and almost close to zero. In the usual Kondo lattice compound with antiferromagnetic ordering, it is enhanced by one order in magnitude. The crystal structure contains two molecules of CePdSb₃, meaning that the number of valence electron is even. This corresponds to a compensated metal with the same number of electrons and holes. The γ value in CePdSb₃ is, however, very small. This might lead to a simple assumption that CePdSb₃ is a semimetal with small volumes of compensated electron and hole Fermi surfaces.

5. Conclusion

To conclude, we have observed bulk antiferromagnetic ordering of Ce moments in an antiferromagnet CePdSb₃. This compound exhibits strongly the anisotropic magnetic susceptibility and isothermal magnetization, reflecting the orthorhombic crystal structure. The magnetization, specific heat and resistivity measurements clearly indicate the antiferromagnetic ordering of CePdSb₃. The grown single crystal has a relatively low-residual resistivity of 5.75 $\mu\Omega\text{-cm}$ at 0.63 K, indicating a highly ordered nature of the crystal. The magnetization

for $H \parallel [001]$ indicates a metamagnetic transition at a low magnetic field of 1.6 kOe and saturates to a value of $1.6 \mu_B/\text{Ce}$ at higher fields, indicating the easy axis of the magnetization, while the $[100]$ direction corresponds to the hard axis. The anisotropic magnetic susceptibility and magnetization were well explained by the CEF model, although we considered only one Ce-site in the analyses.

Acknowledgements

This work was financially supported by the Grant-in-Aid for Scientific Research (A), Scientific Research on Priority Areas and Creative Scientific Research (15GS0213) from the Japan Society of the Promotion of Science and the 21st Century COE Program named "Towards a New Basic Science: Depth and Synthesis".

References

- 1) Y. Ōnuki, T. Goto and T. Kasuya: *Materials Science and Technology* ed. K. H. J. Buschow (Wiley-VCH, Weinheim, 1991) Vol. 3A, Part I, Chap. 7, p. 545.
- 2) Y. Ōnuki and A. Hasegawa: *Handbook on the Physics and Chemistry of Rare Earth*, ed. K. A. Gschneidner Jr. and L. Eyring (Elsevier Science, Amsterdam, 1995) Vol. 20, p. 1.
- 3) T. Hiraoka, E. Kinoshita, H. Tanaka, T. Takabatake and H. Fujii: *J. Magn. Magn. Materials* **153** (1996) 124.
- 4) S. K. Malik and D. T. Adroja: *Phys. Rev. B* **43** (1991) 6295.
- 5) E. D. Bauer, N. A. Frederick, P.-C. Ho, V. S. Zapf, and M. B. Maple: *Phys. Rev. B* **65** (2002) 6295.
- 6) T. Takeuchi, A. Thamizhavel, T. Okubo, M. Yamada, N. Nakamura, T. Yamamoto, Y. Inada, K. Sugiyama, A. Galatanu, E. Yamamoto, K. Kindo, T. Ebihara and Y. Ōnuki: *Phys. Rev. B* **67** (2003) 064403.
- 7) A. Thamizhavel, T. Takeuchi, T. Okubo, M. Yamada, R. Asai, S. Kirita, A. Galatanu, E. Yamamoto, T. Ebihara, Y. Inada, R. Settai and Y. Ōnuki: *Phys. Rev. B* **68** (2003) 054427.
- 8) Y. Inada, A. Thamizhavel, H. Yamagami, T. Takeuchi, Y. sawai, S. Ikeda, H. Shishido, T. Okubo, M. Yamada, K. Sugiyama, N. Nakamura, T. Yamamoto, K. Kindo, T. Ebihara, A. Galatanu, E. Yamamoto, R. Settai and Y. Ōnuki: *Philos. Mag. B*, **82**, (2002), 1867.
- 9) R. J. Cava, A. P. Ramirez, H. Takagi, J. J. Krajewski and W. F. Peck, Jr.: *J. Magn. Magn. Materials* **128** (1993) 124.
- 10) R. T. Macaluso, D. M. Wells, R. E. Sykora, T. E. Albrecht-Schmitt, A. Mar, S. Nakatsuji, H. Lee, Z. Fisk and J. Y. Chan: *J. Solid State Chem.* **177** (2004) 293.
- 11) K. Yamada, K. Yosida and K. Hanzawa: *Prog. Theor. Phys.* **71** (1984) 450.
- 12) K. W. H. Stevens: *Proc. Phys. Soc., London, Sect. A* **65** (1952) 209.
- 13) M. T. Hutchings: *Solid State Physics: Advances in Research and Applications*, edited by F. Seitz and B. Turnbull (Academic, New York, 1965), Vol.16, p.227.